

# Force generation by a parallel array of actin filaments

K. Tsekouras<sup>1</sup>

Physico-Chimie UMR 168, Institut Curie, Paris, France &  
Laboratoire de Physico-Chimie Théorique,  
Ecole Supérieure de Physique et de Chimie Industrielles, Paris, France

D. Lacoste

Laboratoire de Physico-Chimie Théorique,  
Ecole Supérieure de Physique et de Chimie Industrielles, Paris, France

K. Mallick

Service de Physique Théorique,  
Commissariat à l'Energie Atomique- Saclay, Gif, France

J.-F. Joanny

Physico-Chimie UMR 168, Institut Curie, Paris, France

<sup>1</sup>Corresponding author. Address: Institute Curie, 26 rue d'Ulm, Paris, France.  
Tel.:+33(0)156-24-5624, e-mail: konstantinos.tsekouras@curie.fr

## Abstract

We develop a model to describe the force generated by an array of well-separated parallel biofilaments, such as actin filaments. The filaments are assumed to only be coupled through mechanical contact with a movable barrier. We calculate the filament density distribution and the force-velocity relation with a mean-field approach combined with simulations. We identify two regimes: a non-condensed regime at low force in which filaments are spread out spatially, and a condensed regime at high force in which filaments accumulate near the barrier. We confirm that in this model, the stall force is equal to  $N$  times the stall force of a single filament. However, surprisingly, for large  $N$ , we find that the velocity approaches zero at forces significantly lower than the stall force.

*Key words:* force-velocity; actin; stall force; theory

## Introduction

Actin filaments and microtubules are key components of the cytoskeleton of eukaryotic cells. Both play an essential role for cell motility and form the core components of various structures such as lamellipodia or filopodia. They are active elements which exhibit a rich dynamic behavior. For instance, actin filaments treadmill in a process where monomers are depolymerized from one end of the filament while other monomers are repolymerized at the other end. Actin polymerization is highly regulated in the cell, through many actin binding proteins. Some of these proteins accelerate actin polymerization, while others crosslink filaments or create new branches from existing filaments. All these proteins ultimately control the force that a cell is able to produce (1).

In view of this complexity, many experimental studies have focused on biomimetic systems, in which some essential features of biological cells, such as symmetry breaking or motility can be reproduced, in an actin-based system but with a minimal number of proteins (2–4). Additional experiments have been carried out to probe the mechanical properties of the dendritic actin network (5, 6). These experiments have triggered considerable research efforts to model the properties of the actin network and the physical process by which force is generated in such a structure (7–9).

Given the complexity of the actin network, many studies have focused on its basic structural element, namely the filament itself. In order to understand the rich dynamical behavior of single filaments like actin or microtubules, discrete stochastic models have been developed which incorporate at the molecular level the coupling of hydrolysis and polymerization (10–17). These studies also show that the filament internal structure and its age are important features to understand the filament dynamics (18). For instance, hydrolysis is relevant for force generation even at the single filament level, since the force generated by a filament is typically lowered by hydrolysis as shown in (12).

A lower bound for the polymerization force generated by a single actin filament has been deduced from the buckling of a filament which was held at one end by a formin domain and at the other end by a myosin motor (19). An ensemble of parallel filaments is believed to be able to generate larger forces than single filaments, due to interactions between the filaments and load-sharing effects. Such effects arise in parallel bundles, which are present in cellular structures called filopodia. The force generated by a bundle of actin filaments has been measured in (20). At the concentration of actin monomers used in this experiment, the stall force was around 1 pN,

which suggests that the force was in fact supported by a single filament. In a different geometry, the force generated by filaments growing from two magnetic beads outwards has been recently measured (21).

General thermodynamic principles controlling the force produced by the polymerization of growing filaments pushing against a movable barrier were put forward many years ago by Hill et al. (22), but the collective effects in the force generation by several parallel filaments were only modeled much later in studies on the stalling force of microtubules (23–25). In these works, the idea of the brownian ratchet (26) was used at the single filament level, while some specific rule was assumed on how the load is shared by the filaments. Using a detailed balance argument valid only near stalling, it was found that the stall force of an ensemble of  $N$  filaments equals  $N$  times the stall force of a single filament (24). In order to analyze the dependence of the velocity with force away from the stalling point, we revisit in this paper a similar model, namely a model for the force generated by an ensemble of  $N$  parallel filaments with no lateral interaction and no account of hydrolysis.

This paper is organized as follows: we first present the model, present an exact solution in the particular case ( $N = 2$ ) and an approximate solution for the general case of an arbitrary  $N$ . Our analytical approach for this case is compared with simulation results.

## Model

We consider two rigid flat surfaces: one fixed where filaments are nucleated (nucleating wall) and one movable (barrier) whose position is defined to be the position of the filament(s) furthest away from the nucleating wall (thus there is always at least one filament in contact with the barrier). In the cellular environment, this “barrier” is often a membrane against which filaments exert mechanical forces.

We consider an array of  $N$  parallel filaments without any lateral interactions or crosslinkers whether active or passive. We do not model the internal structure of the filaments, and in particular we do not account for ATP hydrolysis. After nucleation, the filaments grow or shrink by exchanging monomers with the surrounding pool of monomers, which acts as a reservoir. The filaments are coupled only through mechanical contact with the barrier. In some previous models (23), a staggered distribution of initial filaments was assumed so that there would be only a single filament in contact at a time. Here we do not make such an assumption, the number of filaments at contact is an arbitrary strictly positive integer. It thus follows that

$T^-(s^{-1})$	$k_0(\mu M^{-1}s^{-1})$	$d(\text{nm})$	$C_c(\mu M)$
1.4	11.6	2.7	0.141

Table 1: Parameters characterizing an actin filament barbed end.  $T^-$  is the free filament depolymerization rate,  $k_0$  is the rate constant entering the free filament polymerization rate  $T^+ = k_0C$ , where  $C$  is the concentration of free monomers,  $d$  is the monomer size and  $C_c$  is the critical concentration.

we can separate the filaments in two populations, the free filaments which are not in contact with the barrier, and the bound filaments which are in contact with the barrier. Only the bound filaments feel the force exerted by the barrier on them, and as a result this changes their polymerization rates as compared with free filaments. We assume that a monomer can be added to any free filament with rate  $T^+$  or removed with rate  $T^-$ , as shown in Fig1. Similarly, a monomer can be added to a bound filament with rate  $v^+$ , and removed with a rate  $v^-$  (or  $T^-$  as explained below). The values of the rates which we have used correspond to an actin barbed end and are given in table 1. We also assume that the barrier exerts a constant force  $F$  on the bound filaments, this force is defined to be positive when the filaments are compressed.

We need now to specify more precisely how the force exerted by the barrier is shared by the bound filaments. When a monomer is added to a bound filament, the barrier moves by one unit, but only the filament on which the monomer has been added does work; we therefore treat all the other filaments as free during that step. Similarly, during depolymerization, filaments depolymerize from the barrier with the free depolymerization rate  $T^-$  as long as there is at least one other filament in contact with the barrier, since in this case the depolymerizing filaments do not produce work. The depolymerization occurs with a rate  $v^-$  only when there is a single filament in contact with the barrier. In this case the filament produces work, since its depolymerization leads to the motion of the barrier.

Since only a single filament carries the load at a time, we can use a form of local detailed balance (27) to relate the rate of addition/loss of monomers from that filament:

$$\frac{v^+}{v^-} = \frac{T^+}{T^-} e^{-f}, \quad (1)$$

which in turn implies the following parametrization of the rates

$$v^+ = T^+ e^{-f\gamma} \quad \text{and} \quad v^- = T^- e^{f(1-\gamma)}, \quad (2)$$

where  $\gamma$  is the “load factor” and  $f$  is the normalized force  $f = Fd/kT$ , where  $d$  is the monomer length. Note that  $\gamma$  itself should be a function of the force, however in the following we assume that it is constant.

An essential feature of this model is that the force only affects the polymerization of a single filament at a time. In the classification of (28), this corresponds to a scenario with “no load sharing”. If the force could be shared by more than one filament, the above discussion would still apply: in this case a single filament would carry a fraction of the load at a time, and for that filament a similar local detailed balance would hold. In this case, although the stalling force would be the same as in the “no-load sharing” scenario, the form of the force-velocity curve would be affected. Such models have been considered in Refs. (24, 25, 28), but for simplicity, in the present paper, we focus on the “no load sharing” model.

## Theory

In this section, we present an analytical exact solution of the model for the case  $N = 2$  and an approximate mean-field solution for the general case  $N > 2$ .

### The particular case of $N = 2$ filaments

Let us call  $p(n, t)$  the probability that there is a gap of  $n$  monomers between the two filament ends at time  $t$ . This quantity satisfies the following equations: for  $n > 1$ ,

$$\frac{\partial p(n, t)}{\partial t} = (v^+ + T^-)[p(n-1, t) - p(n, t)] + (v^- + T^+)[p(n+1, t) - p(n, t)], \quad (3)$$

$$\frac{\partial p(1, t)}{\partial t} = 2(v^+ + T^-)p(0, t) - (v^+ + T^-)p(1, t) + (v^- + T^+)[p(2, t) - p(1, t)], \quad (4)$$

$$\frac{\partial p(0, t)}{\partial t} = (v^- + T^+)p(1, t) - 2(v^+ + T^-)p(0, t). \quad (5)$$

In a steady state, Eq. 3 which holds for  $n > 1$ , admits a time independent solution of the form  $p(n) = p(1)\beta^{n-1}$ . The normalization condition for the probabilities  $p(n)$  imposes that  $\beta = (v^+ + T^-)/(v^- + T^+)$ , and then Eqs. 4-5 can be used to fix the value of  $p(0)$ .

Let us define  $q$  as the probability for a single filament to be bound. We find that

$$q = 1 - p(0) = \frac{2(v^+ + T^-)}{v^+ + v^- + T^+ + T^-}. \quad (6)$$

Another quantity of interest is the average number of bound filaments  $N_0$ :

$$N_0 = 2p(0) + \sum_{n=1} p(n) = \frac{2(v^- + T^+)}{v^+ + v^- + T^+ + T^-}, \quad (7)$$

where the average is done with respect to cases where the two filaments are in contact (when  $n = 0$ ) and cases where only one of them is in contact (when  $n > 0$ ).

### An ensemble of $N$ filaments with $N > 2$

The above approach is limited to the  $N = 2$  case because in that case there is a single gap between the filaments. For  $N > 2$ , there are many gaps, so in general such an approach quickly becomes as complicated as the one based on the filaments themselves. In view of this difficulty, we do not seek here an exact solution of the problem, but we rely instead on a mean-field description. Let us define  $N_i$  as the number of filament ends, which are present at a distance  $i$  from the barrier, with the convention that  $i = 0$  corresponds to the barrier itself. Since each filament has only one active end and the total number of filaments is fixed to be  $N$ , we have the condition that  $\sum_{i=0} N_i = N$ . The  $N_i$  obey the following equations:

$$\frac{dN_i}{dt} = (T^- + v^+ N_0)N_{i-1} + (T^+ + v^- q)N_{i+1} - (T^- + T^+ + v^+ N_0 + v^- q)N_i, \quad (8)$$

$$\frac{dN_1}{dt} = (T^+ + v^- q)N_2 - (T^+ + T^- + v^- q + v^+ N_0)N_1 + [T^-(1-q) + v^+(N_0-1)]N_0, \quad (9)$$

$$\frac{dN_0}{dt} = (T^+ + v^- q)N_1 - [v^+(N_0-1) + T^-(1-q)]N_0, \quad (10)$$

where  $q$  represents, as in the previous section, the average probability that there is only a single bound filament. Note that  $q$  is a central quantity in this mean-field approach; it obeys the following self-consistent equation :

$$q = \langle \delta_{N_0=1} \rangle. \quad (11)$$

In Eq. 8, the first term on the r.h.s. represents the contribution of a filament end going from position  $i - 1$  to  $i$ , either because that filament loses a monomer or a monomer is added on one of the bound filaments, thus pushing the barrier away. The second term on the r.h.s. represents the contribution of a filament end going from the position  $i + 1$  to  $i$ , either because that filament gains a monomer or because there is a single filament

in contact with the barrier, which undergoes depolymerization allowing the barrier to come closer. Finally the last term represents the contribution of a filament end going from position  $i$  to position  $i - 1$  or  $i + 1$  either by adding or losing a monomer to itself or because the barrier moves forward (as a result of one monomer been added to one of the bound filaments) or backward (as a result of the depolymerization of the last bound filament). The remaining two equations are also derived in a similar manner.

At steady state, Eq. 8 which holds for  $i \geq 2$ , leads to a time independent solution of the form

$$N_i = N_2 \exp(-(i - 2)/l), \quad (12)$$

where  $l$  is the correlation length (expressed in number of subunits) given by

$$l = \left[ \ln \left( \frac{T^+ + v^- q}{T^- + v^+ N_0} \right) \right]^{-1}. \quad (13)$$

The other two equations Eqs. 9-10, together with the normalization condition fix  $N_2, N_1$  and  $N_0$ . We find that the average number of filaments in contact with the wall  $N_0$  is:

$$N_0 = \frac{(T^+ + v^- q - T^-)N}{T^+ + v^+(N - 1) + (v^- - T^-)q}. \quad (14)$$

When  $N = 2$ , this mean-field solution agrees with the exact solution derived in the previous section only with the additional condition that  $\gamma = 1$ , in which case the on-rate carries all the force dependence. For an arbitrary value of  $\gamma$ , the mean-field solution does not agree with the exact result obtained for  $N = 2$ . This is expected since the mean-field approximation should work well only in the limit of large  $N$ .

The average velocity of the moving barrier is

$$V = d(v^+ N_0 - v^- q), \quad (15)$$

where the first term within the parenthesis is the contribution of the bound filaments polymerizing with rate  $v^+$  and the second term is the contribution from depolymerizing events of a single bound filament. We have not found a way to solve in general the self-consistent equation satisfied by  $q$ , namely Eq. 11, except near stalling conditions as explained in the next section. For this reason, we have calculated numerically  $q$  from simulations, and derived predictions from the mean-field theory assuming that  $q$  is known. For instance, using Eqs. 14 and 15, one obtains the average velocity.



## Results and discussions

### Numerical validation of the mean-field approach

We have tested the validity of the mean-field approach using numerical simulations. We used the classical Gillespie algorithm (29) incorporating the Mersenne Twister random number generator. Runs were executed for  $N$  up to 5000. Up to 200 trial runs were used to derive averages and distributions. We validated the simulation results by comparing them with the particular cases  $N = 1$  and for  $N = 2$  for which an exact solution is known (it is given in (12) for  $N = 1$  and in the previous section for  $N = 2$ ).

By evaluating the parameter  $q$  from the simulations, we obtained a very good agreement between the theoretical approach based on the use of mean-field and the simulations for the determination of the force velocity curve (shown in Fig. 2) and for the number of filaments  $N_0$  in contact with the barrier (shown in Fig. 3). We find that the values of  $N_i$  as determined by theory does not deviate from the simulation value by more than one.

### Condensation transition as function of the applied force

At low forces, the barrier velocity is close to its maximum value given by the free polymerization velocity. In this case, only one or a small number of filaments are bound, therefore  $q \simeq 1$ , which corresponds to a *non-condensed or single filament* regime. The steady state density profile of the filaments is broad as shown in Fig. 4 and the corresponding correlation length is large. With the parameters values corresponding to this figure, we have  $l \simeq 151\text{nm}$ .

Inversely, at high forces, the filaments accumulate at the barrier. As a result  $q \simeq 0$ , the density profile is an exponential as shown in Fig. 5 with a very short correlation length of the order of a monomer size. With the parameters values corresponding to this figure, we have  $l \simeq 4.1\text{nm}$ . Since in this case, the number of bound filaments,  $N_0$  is a finite fraction of  $N$ , we call this regime the *condensed regime*. In this high force regime (typically near the stall force  $F = F_{stall}$ ), since  $F_{stall}d/k_B T \ll 1$ , we have  $Nv^+ \ll T^+$  and  $q \simeq 0$ . In this case, Eq. 14 simplifies to

$$N_0 = \left(1 - \frac{T^-}{T^+}\right) N. \quad (16)$$

This equation can be used to predict the finite fraction of bound filaments in the condensed regime. This condensed regime corresponds to the plateau in the curve of  $N_0$  vs.  $F$  which is shown in Fig. 3. In the conditions of

this figure, Eq. 16 predicts a plateau for  $N_0 \simeq N/2 = 50$  which is indeed observed, and as expected the plateau in  $N_0$  (Fig. 3) occurs at the same force at which the velocity approaches zero (Fig. 2).

### Theoretical stalling force

Let us first discuss here the theoretical expression of the stall force and then in the next section the practical way this limit is approached. The stall force is defined as the value of the force applied on the barrier for which the velocity given by Eq. 15 vanishes. For  $N = 1$ , the stall force is  $F_{stall}^{(1)} = k_B T \ln(T^+/T^-)/d$ . For  $N = 2$ , using the results obtained above for  $N_0$  and  $q$ , we find that the stall force  $F_{stall}^{(2)}$ , is exactly twice the stall force of a single filament,  $F_{stall}^{(1)}$ ,

$$F_{stall}^{(2)} = 2F_{stall}^{(1)} = 2\frac{k_B T}{d} \ln\left(\frac{T^+}{T^-}\right). \quad (17)$$

In the general case of an arbitrary number of filaments  $N$ , we expect that stall force  $F_{stall}^{(N)}$  should be (24, 25):

$$F_{stall}^{(N)} = N\frac{k_B T}{d} \ln\frac{T^+}{T^-}. \quad (18)$$

This result can be derived from the following argument: near stalling conditions, the average density of filaments at contact  $N_0/N$ , can be obtained from Eq. 16 above. This quantity can be used as an approximation of the probability to have one filament in contact when  $N_0/N \ll 1$ . Since  $q$  is the probability that there is a single bound filament (in other words, there is one filament among  $N$  bound and the remaining  $N - 1$  are free), it follows that

$$q = \frac{N_0}{N} \left(1 - \frac{N_0}{N}\right)^{N-1}, \quad (19)$$

which leads using Eq. 16 to

$$q = N \left(1 - \frac{T^-}{T^+}\right) \left(\frac{T^-}{T^+}\right)^{N-1} \simeq N_0 \left(\frac{T^-}{T^+}\right)^{N-1}. \quad (20)$$

We note that Eq. 19 also means that

$$q \simeq N_0 \exp(-N_0), \quad (21)$$

which corresponds to a Poisson statistics for the distribution of the number of filaments at contact. Now reporting the final expression for  $q$  of Eq. 20

into the stalling condition, namely the vanishing of the velocity given by Eq. 15, one obtains the theoretical stalling force given in Eq. 18.

The theoretical expression of the stall force given by this equation is independent of the load distribution factor  $\gamma$ , although this parameter modifies the form of the force-velocity relation, as we have confirmed in our numerical simulations (not shown). The stall force is also not much affected by changes in free monomer concentration (see Fig.6), as expected from the weak logarithmic dependance of Eq. 18. In Fig. 7, the value of  $q$  determined from the simulations is compared with theoretical expression given by Eq. 19 or Eq. 21 (both expressions give similar results). We note that the deviation between the simulation points and the theory increases as the force is lowered, this is due to the mean-field nature of the theory which becomes invalid when the force is small since then the fluctuations are large. For completeness, we also show in Fig. 8 the PDF of the number of filaments at contact for various forces.

### The approach to stalling

Let us now discuss more precisely how the velocity approaches zero. As shown in Fig. 9, we have confirmed that the velocity is indeed exactly zero at the theoretical stall force, in agreement with the theory. But we find that surprisingly in our simulations, for  $N$  larger than about 10, the velocity approaches zero at forces significantly lower than the stall force as shown in Fig.2. We note that a similar effect has been obtained when analyzing the stall force of an ensemble of interacting molecular motors (30). We therefore define an *apparent* stall force, as the value of force where the velocity drops to less than a small fraction  $\alpha = 2.5\%$  of the value it has for zero force (28). In the experimental situation, this bound could correspond for instance to the limit of resolution in the velocity measurement.

The value of the velocity at zero force corresponds to the maximum velocity. When  $F = 0$ , there is no coupling between the filaments, which behave as independent random walkers. The probability to have more than one walker at the leading position is zero in the long time limit, which implies  $q = 1$ . Therefore,  $N_0 = 1$  and the velocity at zero force equals the polymerization velocity of a single filament:

$$V(F = 0) = d(T^+ - T^-), \quad (22)$$

which is mainly controlled by the monomer concentration as shown in Fig. 6. Now using the expression of the velocity at an arbitrary force given by Eq. 15,

the expression of  $N_0$  given in Eq. 14 and the parametrization of the rates of Eq. 2 for the particular case  $\gamma = 1$ , we find that

$$f_{app}^{(N)} = \frac{k_B T}{d} \ln \frac{(1 - \alpha)(T^+ - T^-)N + \alpha T^+ - (\alpha - q)T^-}{\alpha T^+ - (\alpha - q)T^-}. \quad (23)$$

Since  $q \ll 1$  near stalling, we can write the following more explicit expression

$$F_{app}^{(N)} \simeq \frac{k_B T}{d} \ln \left( 1 + \frac{N}{\alpha} - N \right), \quad (24)$$

In Fig.10, we show the apparent stall force given by Eq. 23 as function of  $N$  together with the theoretical stall force of Eq. 18.

To summarize, we have shown in this figure and more generally in this section that the apparent stall force, does not scale linearly with  $N$  as the theoretical stalling force but rather as  $\ln(N)$ . The apparent stalling force is the quantity of experimental interest, it is also near the apparent stalling force that the condensation transition discussed in a previous section occurs (nothing special of that sort occurs near the theoretical stalling force).

## Conclusion

In this paper, we have investigated the dynamics of an ensemble of  $N$  parallel filaments with no lateral interaction, which are exerting a force against a movable barrier. We have constructed a mean-field theory for this problem, which can only be solved exactly in particular simple cases such as  $N = 1$  and  $N = 2$ . We validated our approach for the general case using simulations. We identify two regimes: a non-condensed regime at low force in which filaments are spread out spatially, and a condensed regime at high force in which filaments accumulate near the barrier. The transition occurs near the apparent stalling force where the velocity approaches zero. Surprisingly, for large  $N$ , we find that this regime where velocity approaches zero occurs at forces significantly lower than the theoretical stall force, given by  $N$  times the stalling force of one filament. We find that the apparent stall force does not scale linearly with  $N$  unlike the theoretical stall force.

Several extensions of our work are possible. For instance, bundles can be formed experimentally by growing filaments in the presence of specific proteins which cross-link the filaments. To describe such a situation, it would be necessary to include lateral interactions. We expect that a bundle would be characterized by a higher stall force in the presence of lateral interactions.

Another direction, which we have not explored, has to do with the effect of load sharing. As mentioned above, we have analyzed a model in which there is essentially no load sharing, since a single filament carries all the force at a time. It would be interesting to explore more systematically the effect of sharing the load over a larger number of filaments as in (28), while still respecting a form of detailed balance constraint. Although we are likely to observe a different dynamics in this case, we expect that the basic effect associated with the presence of a condensation transition as function of the applied force, should still be present.

Another direction for future study would be incorporate a time dependent force, which would be relevant to experiments such as (20) and (6). Although a time-dependent force could be included in the present model, this modification would not be sufficient to account for some aspects of these experiments which show load history dependence. To account for these, a more refined model incorporating the buckling or branching of the filaments is likely to be necessary, since these effects are expected to play an important role in the description of the mechanical properties of actin gels in experimentally relevant situations. In the end, our model offers a very simplified view of the problem of force generation by actin filaments, but precisely for this reason we hope that it can be a useful starting point for more refined studies.

## Acknowledgements

The authors would like to thank A.B. Kolomeisky, P. Sens, R. Pandinhateeri for stimulating discussions, and J. Baudry for a careful reading of the manuscript. K. Tsekouras would also like to thank J. Elgeti for his help with computational issues. This work has been supported by the ANR (french national research agency) under contract ANR-09-PIRI-0001-02.

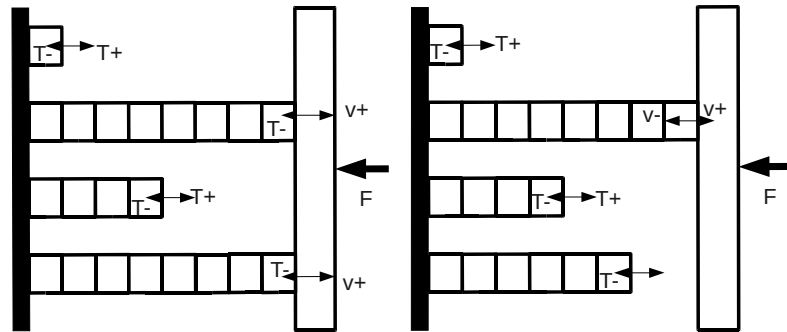


Figure 1: Representation of the filaments pushing on a barrier (the white vertical rectangle on the right, which exerts a force  $F$  on the filaments). The right figure corresponds to the case that only one filament is in contact with the barrier while the left figure corresponds to the case where several filaments are in contact with the barrier. The on and off rates of monomers onto free filaments are  $T^+$  and  $T^-$ . The on-rate on bound filaments is  $v^+$ , and the off-rate is  $v^-$  when there is only one bound filament and  $T^-$  otherwise.

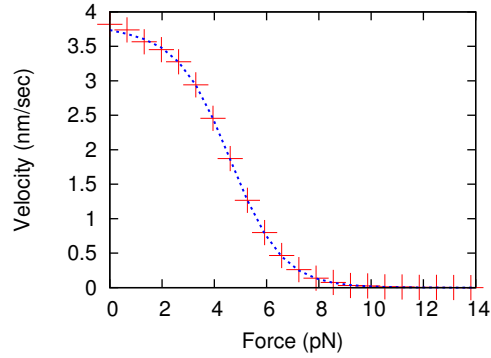


Figure 2: Average barrier velocity vs. force for  $N = 100$  filaments, load factor  $\gamma = 1$  and a free monomer concentration  $C = 0.24\mu M$ . The simulation points are represented as symbols, and the dotted line is the mean-field prediction based on Eq. 15.

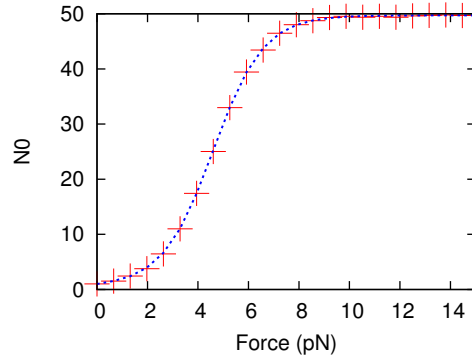


Figure 3: Average number of filaments in contact with the barrier in the same conditions as for Fig. 2. The simulation points are represented as symbols, and the dotted line is the mean-field prediction based on Eq. 14.

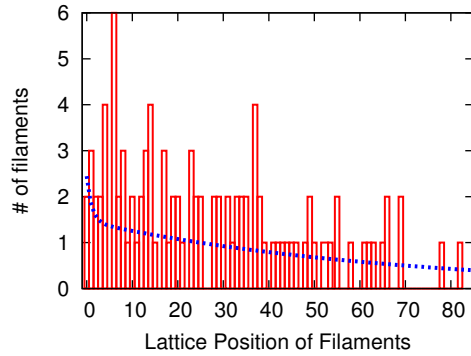


Figure 4: Density profile in the non-condensed regime (shown with bars) as function of the distance to the barrier, together with the prediction from the mean-field theory (shown as a dotted line) from Eq. 12. The parameters are  $F = 2pN$ ,  $N = 100$ ,  $\gamma=1$ ,  $C=0.24\mu\text{M}$ , the force is low with respect to the apparent stall force  $\approx 12pN$ .

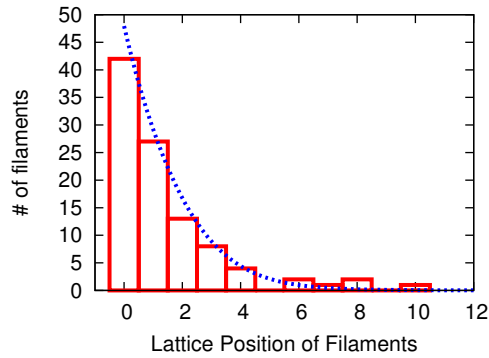


Figure 5: Density profile in the condensed regime (shown with bars) as function of the distance to barrier, together with the prediction from the mean-field theory (shown as a dotted line) from Eq. 12. The parameters are  $F = 12pN$  (close to the apparent stall force),  $N = 100$ ,  $\gamma=1$ ,  $C=0.24\mu\text{M}$ .



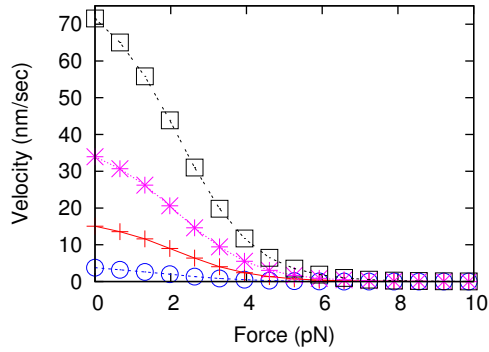


Figure 6: Average barrier velocity as function of the force  $F$  in pN for different monomer concentrations. Note that  $N = 10$  and  $\gamma=1$ . The symbols correspond to different monomer concentrations:  $C = 0.24\mu\text{M}$  (circles),  $0.6\mu\text{M}$  (crosses),  $1.2\mu\text{M}$  (stars) and  $2.4\mu\text{M}$  (squares).

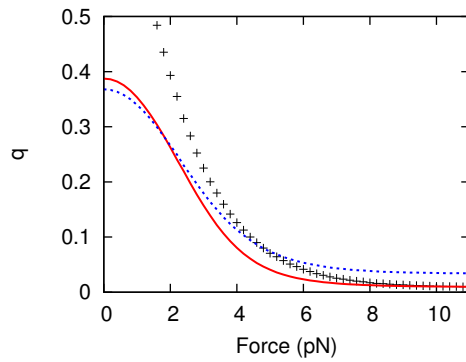


Figure 7: Comparison between theoretical and numerical estimates for the parameter  $q$ , which represents the probability that there is a single bound filament. The plus symbols are simulations points, the dotted line corresponds to Eq. 21 and the continuous line is Eq. 19 (both expressions are mean-field approximations valid in the high force regime). The parameters are  $N = 10$ ,  $\gamma = 1$  and  $C = 0.24\mu\text{M}$ .

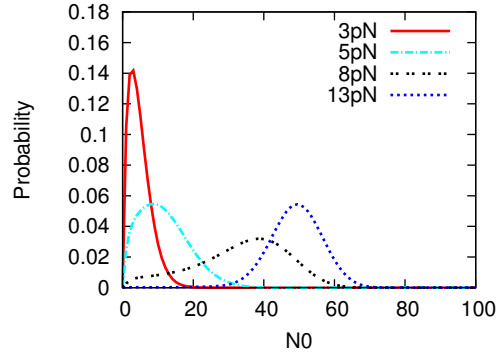


Figure 8: Probability distributions of the number of filaments in contact with the barrier at various forces. The parameters are  $N = 100, \gamma = 1$  and  $C = 0.24 \mu M$ .

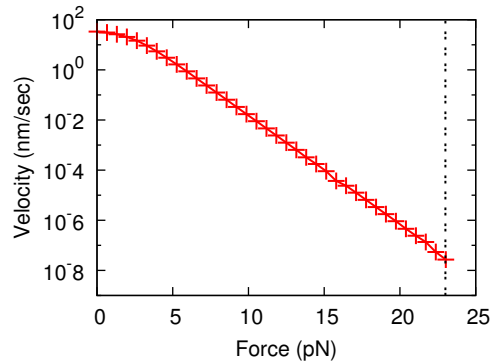


Figure 9: Average barrier velocity near stalling in logarithmic scale. Note that the velocity decreases to zero exponentially when approaching the theoretical stalling force. The parameters are  $N = 10, \gamma = 1$  and  $C = 1.2 \mu M$ .

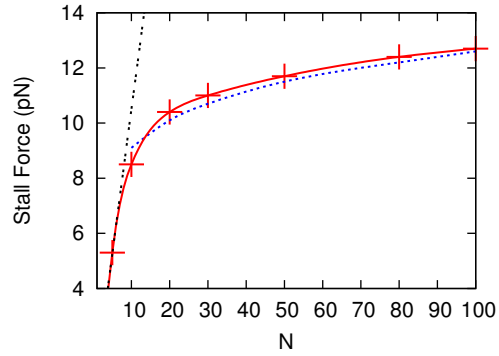


Figure 10: Theoretical stalling force (spaced dotted straight line calculated from Eq. 18) and apparent stalling force as computed from simulations (red symbols) or from the mean-field approximation given of Eq. 23 (dotted line) vs. number of filaments  $N$ . The parameters are  $\gamma = 1$  and  $C = 0.24\mu M$ .

## References

1. Pollard T.D., and J.A. Cooper 2009. Actin, a central player in cell shape and movement. *Science* 326
2. Dayel M.J., O. Akin, M. Landeryou, V. Risca, A. Mogilner and R.D. Mullins 2009. In silico reconstitution of actin-based symmetry breaking and motility. *PLoS Biology* 7:e1000201
3. van der Gucht J., E. Paluch, J. Plastino and C. Sykes 2005. Stress release drives symmetry breaking for actin-based movement. *PNAS* 22:7847-7852
4. Achard V., J.-L. Martiel, A. Michelot, C. Guerin, A.-C. Reymann, L. Blanchoin and R. Boujemaa-Paterski 2010. A “Primer”-based mechanism underlies branched actin filament network formation and motility. *Curr. Biol.* 20:423-428
5. Greene G.W., T.H. Anderson, H. Zen, B. Zappone and J.N. Israelachvili 2008. Force amplification response of actin filaments under confined compression. *PNAS* 106:445-449
6. Fletcher D. 2005. Loading history determines velocity of actin network growth. *Nature Cell Biol.* 7:1219-1223
7. Enculescu M., A. Gholami and M. Falcke 2008. Dynamic regimes and bifurcations in a model of actin-based motility. *Phys. Rev. E* 78:031915
8. Walcott S. and S.X. Sun 2009. A mechanical model of actin stress fiber formation and substrate elasticity sensing in adherent cells. *PNAS* 107:7757-7762
9. Lee K.-C. and A.J. Liu 2009. Force-velocity relation for actin-polymerization-driven motility from brownian dynamics simulations. *Biophys. J.* 97: 1295-1304
10. Stukalin E.B. and A.B. Kolomeisky 2005. Polymerization dynamics of double-stranded biopolymers: Chemical kinetic approach. *J. Chem. Phys.* 122:104903
11. Stukalin E.B. and A.B. Kolomeisky 2006. ATP hydrolysis stimulates large length fluctuations in single actin filaments. *Biophys. J.* 90:2673-2685

12. Ranjith P., D. Lacoste, K. Mallick and J.-F. Joanny 2009. Nonequilibrium self-assembly of a filament coupled to ATP/GTP hydrolysis. *Biophys. J.* 96:2146-2159
13. Ranjith P., K. Mallick, J.-F. Joanny and D. Lacoste 2010. Role of ATP-hydrolysis in the dynamics of a single actin filament. *Biophys. J.* 98:1418-1427
14. Vavylonis D., Q. Yang and B. O'Shaughnessy 2005. Actin polymerization kinetics, cap structure, and fluctuations. *PNAS* 102:8543-8548
15. Antal T., P.L. Krapivsky, S. Redner, M. Mailman and B. Chakraborty 2007. Dynamics of an idealized model of microtubule growth and catastrophe. *Phys. Rev. E* 76:041907
16. Antal T., P.L. Krapivsky and S. Redner 2007. Dynamics of microtubule instabilities. *J. Stat. Mech* 1742-5468
17. X. Li, R. Lipowsky and J. Kierfeld 2010. Coupling of actin hydrolysis and polymerization: Reduced description with two nucleotide states *Eur. Phys. Lett.* 89: 38010
18. Kueh H.Y. and T.J. Mitchison 2009. Structural plasticity in actin and tubulin polymer dynamics. *Science* 325
19. Kovar R.D., and T.D. Pollard 2004. Insertional assembly of actin filament barbed ends in association with formins produces piconewton forces. *PNAS* 41:14725-14730
20. Footer M.J., J.W.J. Kerssemakers, J.A. Theriot and M. Dogterom 2006. Direct measurement of force generation by actin filament polymerization using an optical trap. *PNAS* 104:2181-2186
21. Brangbour C., O. du Roure, E. Helfer, D. Démoulin, A. Mazurier, M. Fermigier, M.-F. Carlier, J. Bibette and J. Baudry. Force velocity measurements of a few growing actin filaments. *in press for PLoS*
22. Hill T.L and M.W. Kirschner 1981. Subunit treadmilling of microtubules or actin in the presence of cellular barriers: Possible conversion of chemical free energy into mechanical work. *PNAS* 79:490-494
23. Mogilner A. and G. Oster 1999. The polymerization ratchet model explains the force-velocity relation for growing microtubules. *Eur. Biophys. J.* 28:235-242

24. Sander van Doorn G., C. Tanase, B.M. Mulder, and M. Dogterom 2000. On the stall force for growing microtubules. *Eur. Biophys. J.* 29:2-6
25. Tanase C., Physical modeling of microtubule force generation and self-organization (PhD Thesis, Wageningen University) 2004.
26. Peskin C.S., G.M. Odell and G.F. Oster 1993. Cellular motions and thermal fluctuations: the Brownian ratchet. *Biophys. J.* 65: 316-324
27. Hill, T.L. 1987. Linear Aggregation Theory in Cell Biology. Springer, Berlin, Germany.
28. Schaus T.E. and G.G. Borisy 2008. Performance of a population of independent filaments in lamellipodial protrusion. *Biophys. J.* 95:1393-1411
29. Gillespie D.T. 1976. A general method for numerically simulating the stochastic time evolution of coupled chemical reactions. *J. Comp. Phys.* 22:403-434
30. O. Campás, Y. Kafri, K. B. Zeldovich, J. Casademunt, and J.-F. Joanny 2006. Collective dynamics of interacting molecular motors. *Phys. Rev. Lettr.* 97:038101
31. Dogterom M. and B. Yurke 1997. Measurement of the force-velocity relation for growing microtubules. *Science* 278:856-860
32. Hu J., A. Mantzavinos and H.G. Othmer 2007. A theoretical approach to actin filament dynamics. *J. Stat. Phys.* 128:111-136
33. Laan L., J. Husson, E.L. Munteanu, J.W.J. Kerssemakers and M. Dogterom 2007. Force-generation and dynamic instability of microtubule bundles. *PNAS* 105:8920-8925